Metabolic Engineering 74 (2022) 11–23

Contents lists available at ScienceDirect

Metabolic Engineering

journal homepage: www.elsevier.com/locate/meteng

Engineering diverse fatty acid compositions of phospholipids in *Escherichia coli*

Wenqin Bai [a,1], Winston E. Anthony [b,1], Christopher J. Hartline [a], Shaojie Wang [a], Bin Wang [b,c], Jie Ning [b,c], Fong-Fu Hsu [d], Gautam Dantas [b,c,e,f,*], Fuzhong Zhang [a,g,**]

[a] Department of Energy, Environmental and Chemical Engineering, Washington University in St. Louis, Saint Louis, MO, 63130, USA
[b] The Edison Family Center for Genome Sciences and Systems Biology, Washington University School of Medicine in St. Louis, Saint Louis, MO, 63110, USA
[c] Department of Pathology and Immunology, Washington University School of Medicine in St. Louis, Saint Louis, MO, 63110, USA
[d] Mass Spectrometry Resource, Division of Endocrinology, Metabolism, and Lipid Research, Department of Medicine, Washington University School of Medicine, St. Louis, MO, 63110, USA
[e] Department of Molecular Microbiology, Washington University School of Medicine in St. Louis, Saint Louis, MO, 63110, USA
[f] Department of Biomedical Engineering, Washington University in St. Louis, Saint Louis, MO, 63130, USA
[g] Institute of Materials Science & Engineering, Washington University in St. Louis, Saint Louis, MO, 63130, USA

A B S T R A C T

Bacterial fatty acids (FAs) are an essential component of the cellular membrane and are an important source of renewable chemicals as they can be converted to fatty alcohols, esters, ketones, and alkanes, and used as biofuels, detergents, lubricants, and commodity chemicals. Most prior FA bioconversions have been performed on the carboxylic acid group. Modification of the FA hydrocarbon chain could substantially expand the structural and functional diversity of FA-derived products. Additionally, the effects of such modified FAs on the growth and metabolic state of their producing cells are not well understood. Here we engineer novel *Escherichia coli* phospholipid biosynthetic pathways, creating strains with distinct FA profiles enriched in ω7-unsaturated FAs (ω7-UFAs, 75%), Δ5-unsaturated FAs (Δ5-UFAs, 60%), cyclopropane FAs (CFAs, 55%), internally-branched FAs (IBFAs, 40%), and Δ5,ω7-double unsaturated FAs (DUFAs, 46%). Although bearing drastically different FA profiles in phospholipids, UFA, CFA, and IBFA enriched strains display wild-type-like phenotypic profiling and growth. Transcriptomic analysis reveals DUFA production drives increased differential expression and the induction of the *fur* iron starvation transcriptional cascade, but higher TCA cycle activation compared to the UFA producing strain. This likely reflects a slight cost imparted for DUFA production, which resulted in lower maximum growth in some, but not all, environmental conditions. The IBFA-enriched strain was further engineered to produce free IBFAs, releasing 96 mg/L free IBFAs from 154 mg/L of the total cellular IBFA pool. This work has resulted in significantly altered FA profiles of membrane lipids in *E. coli*, greatly increasing our understanding of the effects of FA structure diversity on the transcriptome, growth, and ability to react to stress.

1. Introduction

A bacterial cell is a tightly controlled, semi-closed system which is constantly reacting to the effects of an ever-changing environment. The cellular membrane is the first line of cellular defense, compartmentalizing the biochemical processes necessary for cell survival (Zhang and Rock, 2008; Chang and Cronan, 1999). Phospholipids are a major component of cell membranes and play key roles in cell growth, transport, metabolism, survival, and stress tolerance (Zhang and Rock, 2008; Sinensky, 1974; Budin et al., 2018). In Gram-negative bacteria, the fatty acid (FA) profile of lipid membranes mostly consists of straight-chain saturated FAs, with some unsaturated and cyclopropane FAs, while in Gram-positive bacteria, varying amount of terminally branched FAs are observed (Hildebrand and Law, 1964; Bai et al., 2019).

Due to their efficient biosynthesis, microbial FAs have been recognized as important intermediates for the renewable production of biofuels, commodity chemicals, detergents, lubricants, and polymer precursors (Kim et al., 2019; Abraham, 1995; Akhtar et al., 2013; Carroll et al., 2016; Jiang et al., 2017; Steen et al., 2010; Yan and Pfleger, 2020; Peralta-Yahya et al., 2012). Unfortunately, natural microbial FAs exhibit high melting temperatures, making their derived products suffer from undesirable properties, such as for bacterial FA-derived biofuels (Jiang

* Corresponding author. The Edison Family Center for Genome Sciences and Systems Biology, Washington University School of Medicine in St. Louis, Saint Louis, MO, 63110, USA.
** Corresponding author. Department of Energy, Environmental and Chemical Engineering, Washington University in St. Louis, Saint Louis, MO, 63130, USA.
E-mail addresses: dantas@wustl.edu (G. Dantas), fzhang@seas.wustl.edu (F. Zhang).
[1] These authors contributed equally to this work.

https://doi.org/10.1016/j.ymben.2022.08.011
Received 8 February 2022; Received in revised form 15 April 2022; Accepted 26 August 2022
Available online 1 September 2022

et al., 2017; Lee et al., 2008; Tao et al., 2015). Bacteria exhibit the ability to adapt to different environments and growth stages by altering the composition of their phospholipid FAs (Cronan, 2002; Willdigg and Helmann, 2021). *Escherichia coli ML30*, for example, increases the proportion of unsaturated FAs from 47% to 62% when the temperature drops from 37 °C to 10 °C (Sinensky, 1974). Modulating membrane composition is an established bioengineering concept called membrane engineering and has even been used to increase *E. coli* tolerance to bioproducts such as carboxylic acids, alcohols, and aromatic compounds, as well as adverse conditions, such as low temperature (Tan et al., 2016; Dunlop, 2011). Expanding the diversity of bacterial produced FA-derived products would increase their applicability and value but necessitates methods to predictably modify the chemical structure of FA species.

Previous work on engineering free FA (FFA) pathways focused on modifying the carboxylic acid group (Steen et al., 2010; Schirmer et al., 2010; Goh et al., 2012; Nawabi et al., 2011) and the ω-terminal carbon to other functional groups (Bowen et al., 2016; Jiang et al., 2015a; Bentley et al., 2016), or modulating the chain-length of FFAs (Lennen and Pfleger, 2013). In comparison, altering the internal FA hydrocarbon chain can provide a new class of renewable compounds for various applications, but this has been seldom explored. This is potentially because enzymes responsible for modifying internal hydrocarbon chains only use phospholipid FAs as substrates (Zhang and Rock, 2008; Grogan and Cronan, 1997), and modifying the membrane phospholipid can have significant detrimental effects to cell growth and viability under stressful conditions (Rowlett et al., 2017). For example, lipid incorporation of medium-chain FAs that are shorter than native FAs can lead to membrane damage and drastically reduce cell viability (Lennen et al., 2011; Royce et al., 2013). Similarly, incorporation of exogenously-fed, non-native polyunsaturated FAs into membrane phospholipids can change expression of genes related to cellular respiration, membrane integrity, and oxidative stress (Hobby et al., 2019). Increasing unsaturated FAs (UFAs) in *E. coli* has been attempted before, however the limited structural diversity of naturally produced UFAs has relegated these efforts to monounsaturated FAs and cyclopropane FAs (CFAs) (Budin et al., 2018; Cao et al., 2010, 2014).

In this study, we introduce engineered phospholipid biosynthetic pathways into the *E. coli* chassis to produce bacterial strains with greatly diversified, yet highly controllable FA profiles, resulting in FA compositions substantially different from that of the native cell. These strains are enriched in ω7-unsaturated fatty acids (ω7-UFAs; C16:1,Δ9 and C18:1, Δ11), cyclopropane fatty acids (CFAs; C17:0, cyclo9 and C19:0, cyclo11), Δ5-monounsaturated fatty acids (Δ5-MUFAs; C16:1, Δ5), doubly unsaturated fatty acids (DUFAs; C16:2, Δ5Δ9 and C18:2, Δ5Δ11), or internally-branched fatty acids (IBFAs; C17:0 Me10 and C19:0 Me12), with later three types of FAs non-native to *E. coli* (Fig. 1). The produced DUFAs and IBFAs (structurally different from tuberclostearic acid, C19:0 Me10) are extremely rare in nature and have only been identified in trace amounts from the seed of the *Ephedra* plant and from sulfide-forming bacteria, respectively (Wolff et al., 1999). We further investigate the effect of modifying cell FA composition on bacterial growth, viability in stressful conditions, and on the metabolic networks of the cell. CFA- and IBFA-enriched strains exhibited similar growth rates, cell densities, and responses to environmental stress as wild-type *E. coli* under a wide range of conditions. DUFA enrichment resulted in reduced viability across multiple environmental conditions, a markedly different transcriptomic profile, as well as lowered cell densities in glycerol and glucose supplemented with high salt. These designed strains substantially diversify phospholipid FA composition within *E. coli*, and through the demonstrated production of free IBFAs (FIBFAs) create new opportunities in biotechnology as microbial hosts for chemical production (Tan et al., 2016).

2. Results

2.1. Engineering E. coli to modulate phospholipid profile

Wild-type *E. coli* K-12 strains contain 30–60% UFAs with a *cis* double bond located precisely at the ω7 position (ω7-UFAs) (Bai et al., 2019)' (Marr and Ingraham, 1962)' (Cronan and Gelmann, 1973). ω7-UFAs can be used as intermediates for synthesizing other FA structures such as CFA and internally branch-chain fatty acids (IBFAs) (Bai et al., 2019; Shuntaro et al., 2017; Taylor et al., 1981). Accordingly, we started by engineering *E. coli* to enrich ω7-UFAs in phospholipids. The FA degradation pathway was first deactivated by deleting *fadE*, whose enzyme product catalyzes the first step in β-oxidation (Yan and Pfleger, 2020). To create a strain that produced only ω7-UFAs in addition to saturated

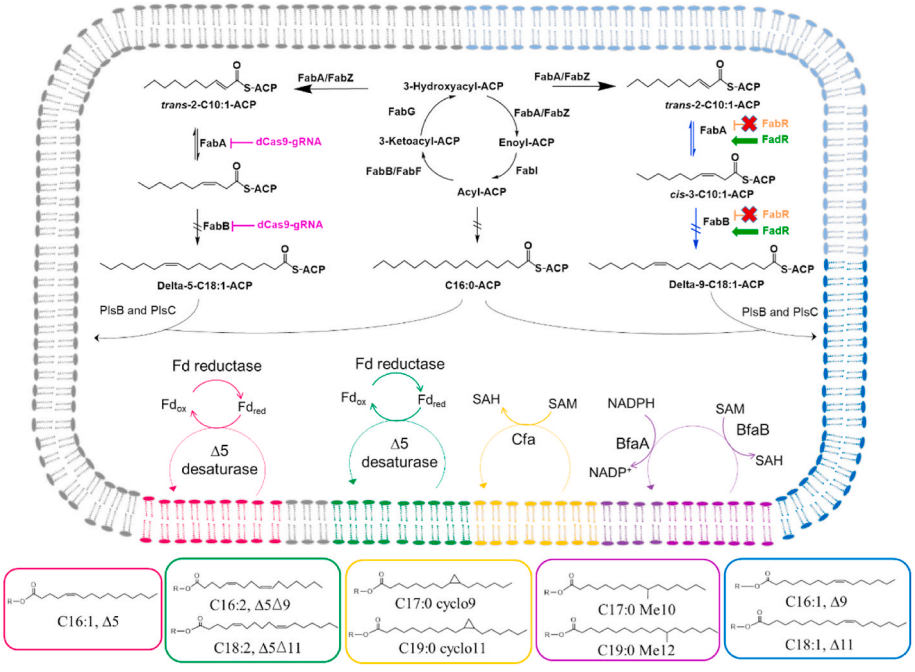

Fig. 1. Engineered pathways for the biosynthesis of different FAs in membrane phospholipids in *E. coli*. Each type of FAs is boxed in the same colored as their biosynthetic pathways. FabA or FabZ: β-hydroxyacyl-ACP dehydrase; FabB: β-ketoacyl-acyl ACP synthase I; FabF: β-ketoacyl-acyl ACP synthase II; FabG: β-ketoreductase; FabH: β-ketoacyl-acyl carrier protein (ACP) synthase III; FabI or FabK: enoyl-ACP reductase; PlsB: glycerol-3-phosphate acyltransferase; PlsC: 1-acyl-sn-glycerol-3-phosphate acyltransferase; Fd: ferredoxin; SAM: S-adenosyl-L-methionine; SAH: S-adenosyl-L-homocysteine; BfaA: NADPH dependent oxidoreductase; BfaB: SAM-dependent methyltransferase; Cfa: cyclopropane fatty acid synthase.

straight-chain FAs, the CFA synthase (encoded by *cfa*) that converts ω7-UFA to CFA was deleted from the *E. coli* genome. The resulting strain, named ω7-UFA-1, significantly increased ω7-UFA composition to 50.0 ± 0.4%, in comparison to 31.5 ± 1.2% (student's t-test, adjusted p value = 0.002) in wild-type *E. coli* (Fig. 2a). Next, the FA transcriptional regulator FadR, which activates the expression of two ω7-UFA biosynthesis genes *fabA* and *fabB,* was overexpressed, significantly increasing ω7-UFA composition to 55.8 ± 0.0% (Strain ω7-UFA-2) versus WT (student's t-test, adjusted p value = 0.002). To further enrich ω7-UFA, three strategies were explored in parallel to optimize *fabA* and *fabB* expression. In the first strategy, an additional copy of *fabB* or *fabAB* was overexpressed from a plasmid, which increased ω7-UFA compositions to 75.0 ± 5.2% (student's t-test, adjusted p value = 0.007 versus WT) and 72.0 ± 2.0% (student's t-test, p value = 0.002 versus WT), respectively (Fig. 2a and Fig. S1a). The third strategy involved the deletion of FabR, another FA transcriptional regulator that represses the expression of *fabA* and *fabB*. Deletion of FabR increased ω7-UFA composition to 69.4 ± 1.0% (student's *t*-test, adjusted p value = 0.002). Of these engineered variants, strain ω7-UFA-5 produced the highest ω7-UFA titer, reaching 197.7 ± 16.3 (adjusted p value < 0.05 versus all strains) mg/L (Fig. S1a). The titer achieved in this work is 5.7-fold higher than previous efforts solely relying on overexpression of *fabAB* alone, which do not prevent *cfa* formation (Cao et al., 2010). The enhanced titers presented here may also be attributed to the overexpression of *fadR*, which has been shown to enhance overall titers of FAs through a more global tuning of FA pathway genes (Zhang et al., 2012).

CFAs are naturally synthesized in *E. coli* (Fig. 1) and are important for bacterial resistance to environmental stresses, such as acid and high osmotic pressure (Chang and Cronan, 1999; Shabala and Ross, 2008). However, WT *E. coli* only accumulates between 2 and 20% of CFAs during logarithmic growth (Cronan et al., 1974; Cronan, 1968), and our wild-type *E. coli* only accumulated 12.5 ± 2.3% of CFA in phospholipid when tested. To enhance CFA composition in phospholipid, we overexpressed CFA synthase in the *fadE*-deleted *E. coli* strain and observed an increase in the proportion of CFAs to 39.7 ± 2.2% (p value = 0.006, Student's t-test versus WT), consisting of 29.2 ± 2.4% C17:0 CFA and 10.5 ± 0.6% C19:0 CFA (strain CFA-1, Fig. 2b) as identified by Gas Chromatography-Mass Spectrometry (GC-MS) (Figs. S3a–b). CFA is biosynthesized by methylation of ω7-UFA (Bai et al., 2019). To enhance the cellular pool of ω7-UFA, FabR was deleted and FadR was overexpressed. The resulting strain (CFA-2) produces 53.7 ± 4.5% CFAs and 19.8 ± 4.5% ω7-UFA. *E. coli* Cfa methylates ω7-UFA preferably at the sn-2 position in phospholipids. To convert the remaining ω7-UFA to CFA, the *Clostridium butyricum* Cfa, which prefers the sn-1 position (Hildebrand and Law, 1964), was overexpressed. While overexpression *C. butyricum* Cfa alone produced 19.2 ± 3.9% CFA (strain CFA-3), coexpression of both *E. coli* Cfa and *C. butyricum* Cfa (strain CFA-4) increased CFA composition to 55.3 ± 0.3% (p value = 0.004 Student's t-test versus WT), with a titer of 84.7 ± 4.7 (p value = 0.003 Student's t-test versus WT) mg/L (Fig. S1b).

Internally branched fatty acids (IBFAs) have substantially lower melting temperatures compared to straight-chain FAs of the same length, and are thus attractive precursors for jet-fuels, which demand low freezing points. However, IBFAs are mostly found in *Mycobacterium tuberculosis* and a few other *Mycobacterium* and *Rhodococcus* species (Bai et al., 2019; Machida et al., 2017). To produce IBFAs in *E. coli*, we overexpressed the *R. opacus* PD630 IBFA biosynthetic pathway, which contains a S-adenosyl-l-methionine-dependent methyltransferase (BfaB)

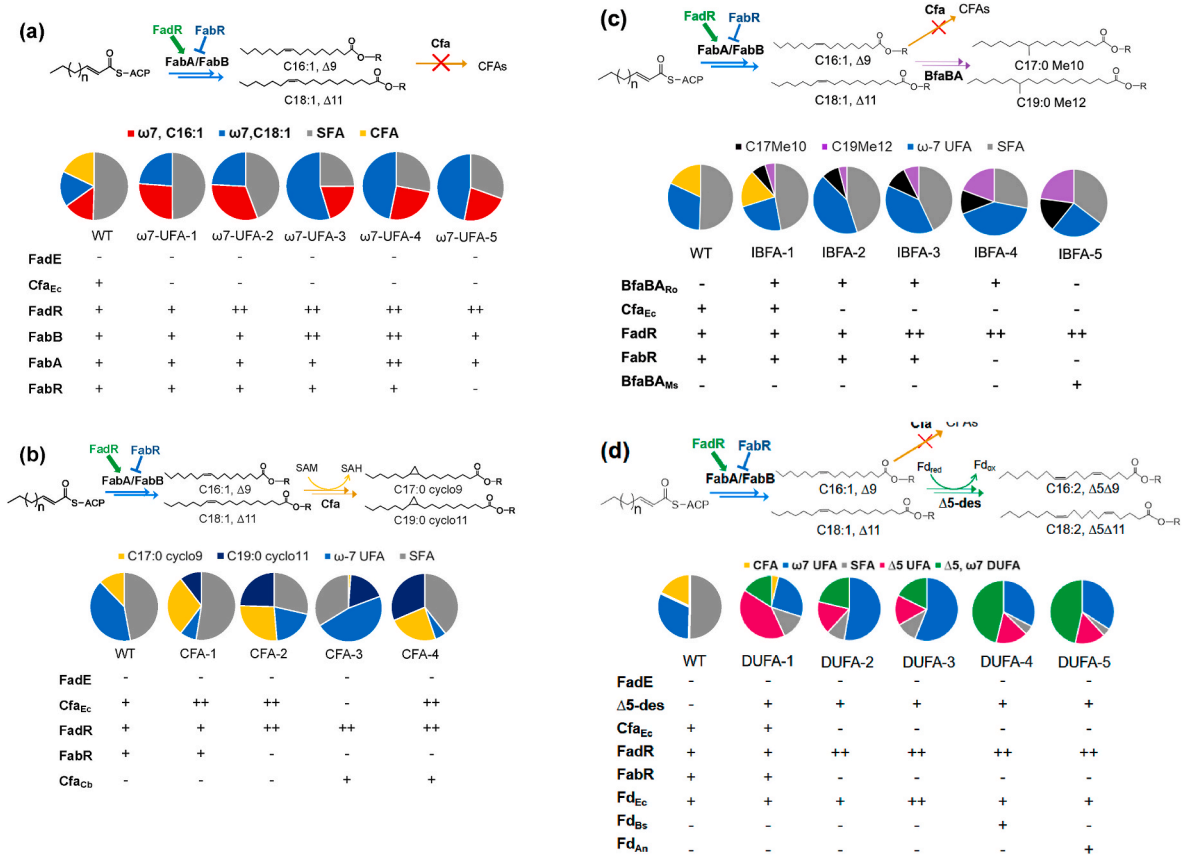

Fig. 2. Engineering *E. coli* to produce ω7-unsaturated fatty acids (ω7-UFAs, **a**), cyclopropane fatty acids (CFAs, **b**), Internally branched fatty acids (IBFAs, **c**), doubly unsaturated fatty acids (DUFAs, **d**), and Δ5-unsaturated fatty acids (Δ5-MUFAs, **e**) in phospholipids. The engineered biosynthetic pathways are shown on the top of each figure. Pie-charts indicate the FA composition in the phospholipid of each strain. Genetic changes for each strain are shown under each Pie-chart. - indicates gene deletion from *E. coli*'s genome; + indicates the native gene is not deleted; ++ indicates gene overexpression from plasmid DNA.

and a FAD-binding oxidoreductase (BfaA) (Bai et al., 2019; Machida et al., 2017). The resulting *E. coli* strain converts palmitoleic acid (C16:1Δ9) and vaccenic acid (C18:1Δ11) to 10-methylhexadecanoic acid (C17:0Me10) and 12-methyl octadecanoic acid (C19:0Me12), respectively, with a total IBFA composition of 11.7% (Strain IBFA-1, average of two replicates, Fig. 2c, Figs. S1c and S4 and S3c-d). To further increase IBFA composition, Cfa was deleted to avoid competition with the ω7-UFA precursor, and ω7-UFA biosynthesis was enhanced by FabR deletion and FadR overexpression. These engineering strategies led to a gradual increase of IBFA composition up to 30.9 ± 1.2% (p value = 2.0E-04, Students t-test versus IBFA-1). Additionally, BfaAB enzymes from different microorganisms were screened. The *Mycobacterium smegmatis* enzymes (strain IBFA-5) produced the highest IBFA composition, up to an average of 39.2 ± 1.2% with an IBFA titer of 91.3 ± 4.6 mg/L (p value = 7.1E-05, Student's *t*-test versus IBFA-1).

Double unsaturated FAs (DUFAs) are intermediates in the biosynthesis of polyunsaturated FAs that have various health benefits due to their abilities in scavenging radical species (Richard et al., 2008). To produce DUFAs in *E. coli*, we overexpressed the Δ5-desaturase (encoded by *Δ5-des*) from *Bacillus subtilis* in the *fadE*-deleted *E. coli* strain. The resulting strain DUFA-1 consists of 16.0 ± 0.2% of Δ5,ω7 DUFA (mostly C18:2, Δ5Δ11, Figs. S3e–f), 26.3 ± 1.2% ω7-UFA, and 40.9 ± 0.7% Δ5 C16:1 UFA (Fig. 2d) Increasing the precursor pool of ω7-UFAs by Cfa deletion, FabR knockout, and FadR overexpression increased Δ5,ω7 DUFA to 21.3 ± 1.0% (p value = 0.007, Student's *t*-test versus DUFA-1) (strain DUFA-2), but at the same time resulting in a high ω7-UFA composition (52.6 ± 0.8%), suggesting that the pathway is limited by the Δ5-desaturase. Δ5-desaturase uses a ferredoxin as an electron donor to reduce C–C single bonds at the Δ5 position (Chazarretacifre et al., 2011). To optimize Δ5-desaturase activity, the ferredoxin gene from *E. coli*, *B. subtilis*, and *Anabaena* sp. 7120 was individually overexpressed. Ferredoxin from either *B. subtilis* (strain DUFA-4) or *Anabaena* sp. 7120 (strain DUFA-5) increased Δ5,ω7 DUFA composition to 45.4 ± 0.6% (p value = 1.58E-05, Student's *t*-test versus DUFA-1) and 44.8 ± 3.8% (p value = 0.002, Student's *t*-test versus DUFA-1) in phospholipid with a titer of 151.3 ± 3.0 mg/L and 153.9 ± 16.2 mg/L, respectively (Fig. 2d, Fig. S1d).

While most monounsaturated FAs (MUFAs) contain the double bond at ω7 position, double bonds at alternative positions, such as Δ5, are rare in nature and have only been found in small amounts (<9%) in *B. subtilis* (Wolff et al., 1999) and in the seeds of *Brassica* species. The unique double bond position may enable region-selective labeling and other chemical modifications on FAs for various applications (Bonamore et al., 2006). To produce Δ5-MUFA, the *B. subtilis* Δ5-desaturase (encoded by *Δ5-des*) was overexpressed in the Δ*fadE*-deleted *E. coli* strain. The resulting strain (Δ5-MUFA-1) contains only 7.8 ± 1.7% of Δ5-MUFAs (Fig. S3g), with 10.4 ± 1.1% of ω7-UFAs and 18.6 ± 1.7% CFAs (Fig. 3c). Deletion of Cfa to eliminate CFAs enhanced Δ5-MUFAs to 39.5 ± 7.4% (p value = 0.0001, Student's *t*-test versus MUFA-1). To further increase the proportion of Δ5-MUFAs, we aimed to decrease ω7-UFA biosynthesis by repressing the expression of *fabA* and *fabB*. As low levels of ω7-UFAs are required for cell growth, we reduced *fabA* and *fabB* expression using CRISPR interference (CRISPRi) (Cronan and Gelmann, 1973; Qi et al., 2013). Small guide RNAs (sgRNAs) targeting four different regions of both the *fabA* and *fabB* operons were designed to search for the most optimal level of repression (Fig. 3a). Constitutively expressed sgRNAs were introduced on a plasmid to ω7-UFA strains harboring a *dCas9* gene. Fermentation of the resulting strains showed that a sgRNA targeting nucleotides 484–504 (approximately the middle) of the *fabB* coding region was the most effective in decreasing ω7-UFA composition (Fig. 3b). This sgRNA was then expressed in the Δ5-MUFA strain. The resulting strain (Δ5-MUFA-3) has 60.0 ± 0.1% of Δ5-MUFA in phospholipid FAs, with only 26.4 ± 0.4% native ω7-UFA. Additional overexpression of ferredoxin from either *E. coli*, *B. subtilis*, and *Anabaena* sp. 7120 reduced Δ5-MUFA composition (Fig. 3c, Fig. S2), suggesting an imbalanced redox potential.

2.2. Phospholipid profile analysis of the IBFA-producing strain

After obtaining diverse FA profiles in phospholipids, it is interesting to know how these uncommon FAs are distributed between different phospholipid species, as that can illuminate the substrate specificity of FA-modifying enzymes. In wild-type *E. coli*, phospholipid biosynthesis starts from acylation of glycerol-3-phosphate at both sn-1 and sn-2 positions to form phosphatidic acid (PA). PA is then converted to CDP-diacylglycerol (CDP-DAG) followed by exchanging the head group to phosphatidylethanolamine (PE, ~70%), phosphatidylglycerol (PG, ~25%), cardiolipin (CL, ~4%), and phosphatidylserine (PS, 0.1% of phospholipid) (Hawrot and Kennedy, 1978) (Fig. 4a) (Rowlett et al., 2017; Parsons and Rock, 2013). While the phospholipid substrates for CFA and Δ5-desaturase have been elucidated in previous studies (Hildebrand and Law, 1964; Altabe et al., 2003; Feng and Cronan, 2009), phospholipid substrates for the IBFA pathway remain unknown. To identify the profiles of IBFA on different phospholipids and their sn-positions, we performed lipid analysis of the IBFA-rich strain (IBFA-5) using liquid chromatography-mass spectrometry (LC-MS/MS). The results showed that there was no detectable IBFA in PA, CDP-DAG, and CL. The percentage of IBFA in PG, was significantly higher than PE, or PS: 57.0% ± 0.17, 41.0% ± 1.01, and 39.1% ± 2.63 (adjusted p values < 0.05) respectively (Fig. 4b).

Further analyses of the sn-positions of IBFAs identified a higher methylation activity at the sn-1 position than that of the sn-2 position for each phospholipid (Fig. 4c). At the sn-1 position, 95.4% ± 0.2 of ω7-UFAs were converted to IBFAs in PG, and 85.0% ± 2.8 and 79.0% ± 0.7

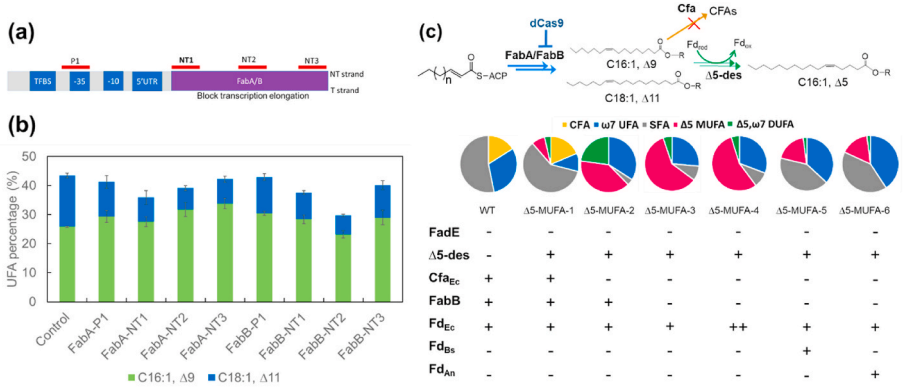

Fig. 3. Engineering *E. coli* to produce Δ5-MUFA in *E. coli*. **a**, sgRNAs bind to different regions of non-template strand of *fabA* or *fabB* gene. **b**, CRISPRi with different sgRNA showed different inhibition efficiency for the production of ω7-UFAs. Targeting of sgRNA to the middle region of *fabB* gene obviously inhibit the production of ω7-UFAs. Error bars represent standard deviation measured from biological triplicates. **c**, The production of Δ5-MUFA in different engineered strains.

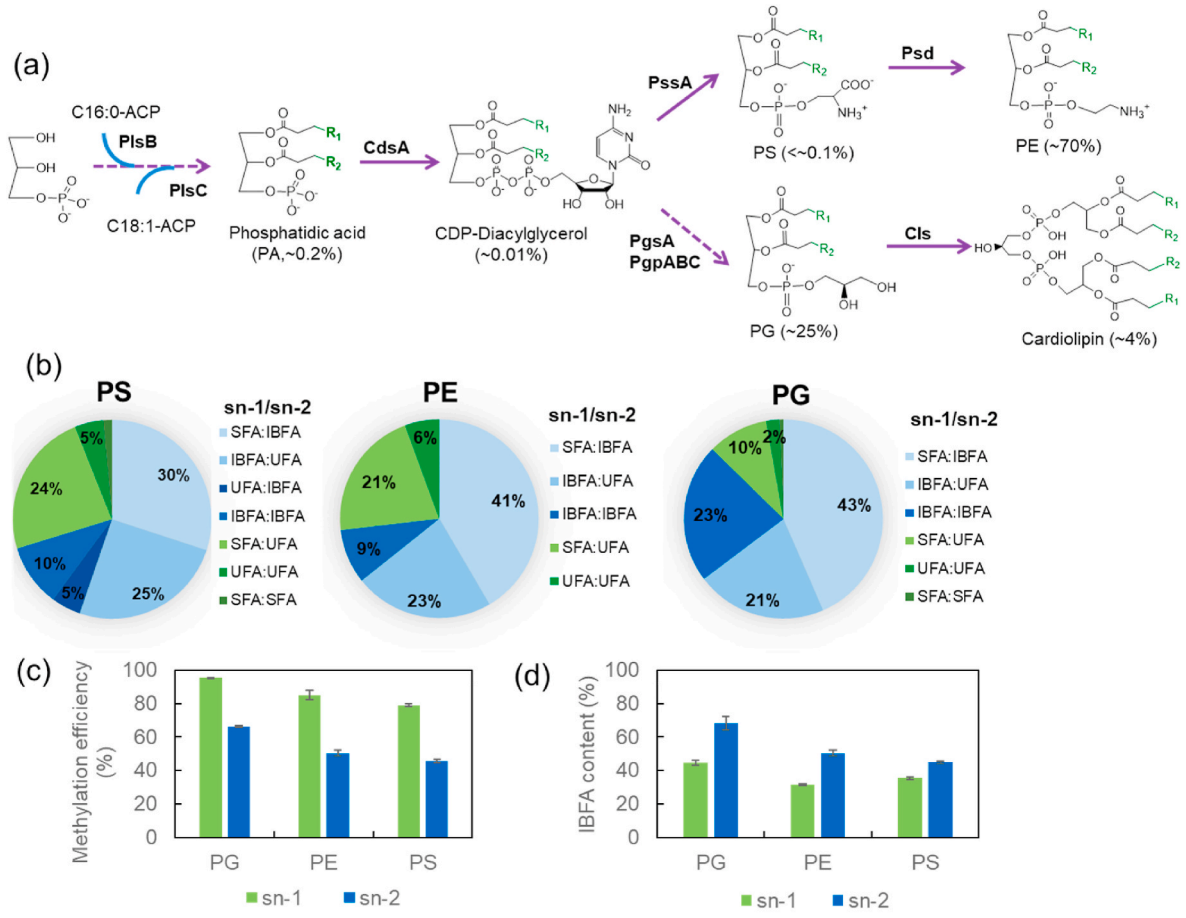

Fig. 4. Lipid profile analysis of the IBFA-enriched strain IBFA-5. **a**, The biosynthesis pathway of major phospholipid species in *E. coli*. **b**, The distribution of IBFA in different phospholipid species in engineered strain. **c**, The methylation efficiency of BfaB as calculated from the ratio of IBFAs to UFA equivalent in different phospholipid species. **d**, The content of IBFAs in different position of different phospholipids. PS: Phosphatidylserine; PE: Phosphatidylethanolamine; Phosphatidylglycerol: Phosphatidylglycerol; Cds: phosphatidate cytidylyltransferase; Pss: phosphatidylserine synthase; Psd: phosphatidylserine decarboxylase; PgsA: phosphatidylglycerolphosphate synthase; PgpA/B/C: phosphatidylglycerolphosphate phosphatase; Cls: cardiolipin synthase; CDP-DAG: cytosine diphosphate-diacylglycerol.

of conversion were obtained for PE and PS, respectively. At the sn-2 position, the ω7-UFA to IBFA conversion ranged from 45.7% ± 1.1, 50.4% ± 1.65, 66.5% ± 0.5 for PE, PG, and PS respectively (Fig. 4c), suggesting the IBFA pathway prefers ω7-UFAs at the sn-1 position of phospholipids. However, the total contents of IBFAs at the sn-1 position (PE = 31.6% ± 0.5, PG = 44.5% ± 1.5, and PS = 35.4% ± 0.9) are lower than that at the sn-2 position (PE = 50.4% ± 1.6, PG = 68.1% ± 4.1, and PS = 45.0% ± 0.7) for each phospholipid (adjusted p values < 0.05) (Fig. 4d).

2.3. Phenotypic profiling of engineered strains with diverse FA profiles

Engineered bioproduction strains often suffer from reduced cell growth and altered metabolism in comparison to their wild-type counterparts (Falls et al., 2014; Oyarzún and Stan, 2013; Dunlop et al., 2010). Here we have created several strains with drastically different FA profiles in phospholipids compared to that of wild-type *E. coli*. We next examined whether these modified FA profiles would affect metabolic activity and cell growth. To test this, we performed phenotype microarrays by cultivating the engineered strains which produced the highest titers of ω7-UFA (ω7-UFA-5), CFA (CFA-4), IBFA (IBFA-5), and DUFA (DUFA-5) in 96 different growth media and conditions such as different carbon sources, organic acids, salts, pH, reducing power, and antibiotics (Fig. S4). Screening of these strains revealed that the IBFA- and CFA-enriched strains have similar growth and metabolic characteristics compared to the control *E. coli* strain without phospholipid FA modification (Fig. 5a, Supplementary Table 4, Supplementary Table 5). Out of the 96 tested growth media and conditions, the IBFA- and CFA-enriched strains have more than 2-fold difference in cell densities in only 5 (reduced growth in 8% NaCl, fusidic acid, vancomycin, lithium chloride, and sodium butyrate) and 1 (sodium bromate) conditions, respectively (Supplementary Table 5). Metabolic activities under these conditions were measured using a tetrazolium redox dye to track oxidative phosphorylation activity. Both IBFA- and CFA-enriched strains exhibited similar metabolic activity to those of the control *E. coli* strain, with only 6.3% and 10.4% of conditions displaying more than 2-fold difference. Interestingly, only the CFA-enriched strain exhibited any increased metabolic activity, under 10 conditions: Dextrin, N-acetyl-β-D-Mannosamine, 3-Methyl Glucose, 1% sodium lactate, L-arginine, L-Glutamic acid, L-Pyroglutamic Acid, Glucuronamide, Quinic acid, D-Lactic acid Methyl Ester (see Supplementary Table 4 for all conditions). Of the 10 conditions with enhanced respiratory activity for CFA, 6 are carbon source conditions which can also be used as a nitrogen source (N-acetyl-B-D-Mannosamine, L-arginine, L-glutamic acid, l-pyroglutamic acid, Glucuronamide), or are amino acid precursors (Quinic acid). This did not correlate with any increased growth in those conditions. The ω7-UFA- and DUFA-enriched strains had reduced metabolic activities and lower cell density for 59.4% (57/96) and 74.0% (71/96) of the tested conditions, respectively.

Additionally, these strains were cultivated in parallel under different

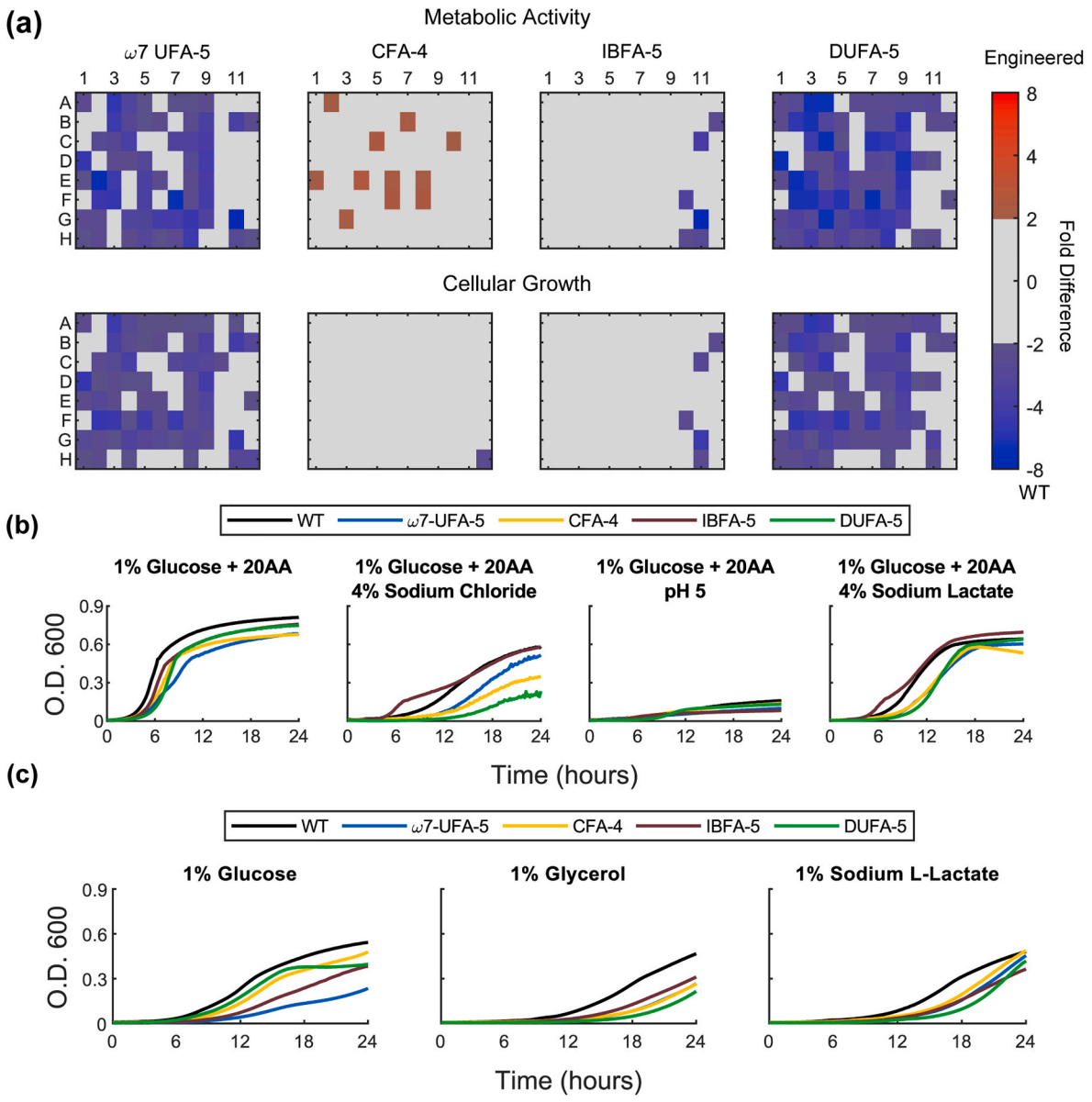

Fig. 5. Phenotypic profiling of engineered strains with diverse FA profiles. **a**, Metabolic activity (top) and Cellular Growth (bottom) across 96 metabolic conditions. Measured Activity is compared against WT strain measured under same conditions. **b&c**, Average growth curves of biological triplicates in select challenge conditions of engineered strains (WT, black; ω7-UFA-5, blue; CFA-4, yellow, IBFA-5, purple; DUFA-5, green).

stress conditions (Fig. 5b, Fig. S5) and in different commonly used carbon sources (Fig. 5c, Fig. S5). Mutant strains reached an estimated maximal growth rate lower than WT when grown in glucose, glucose supplemented with amino acids, and high salt. Mutant strains reached similar maximal growth rates compared to the control strain when grown in glucose supplemented with sodium lactate, sodium L-lactate, or in low pH, or grown in glycerol (Fig. S6, Fig. S7), confirming that these modifications in phospholipid FAs are tolerated by the *E. coli* chassis under controlled laboratory conditions. There were no significant differences between the maximal cell density reached by WT and any of the mutant strains (Fig. S8, Table S6).

2.4. Transcriptomic profiling of engineered strains with diverse FA profiles

Given the aforementioned difference in metabolic burden imposed on the *E. coli* chassis between the IBFA-, CFA-, and DUFA-enriched strains, we next investigated genome-wide expression changes in all strains compared to the UFA-enriched strain (control). To identify the effect of altering FA composition on the transcriptome at different growth phases, we sampled liquid cultures of each strain at 3 time points: 4, 8, and 24 h. A biplot of the principle component analysis of the 500 most variable genes shows that ellipses generated from control, IBFA, and CFA conditions vary along principle component PC2 (Fig. S9). This confirms that the transcriptional state of the UFA, CFA, and DUFA expressing strains were very similar across time (adjusted p value > 0.05 [PERMANOVA], Table S8). The DUFA samples did not follow this relationship, instead varying along PC1, with the DUFA-enriched samples at 4- and 8- hours clustering together away from samples of other strain at similar time points. PERMANOVA comparison of all DUFA samples compared to samples of other strains confirmed a significant difference in variance over time (adjusted p value < 0.05 versus all other strains, Table S8). Additionally, examining the 40 most variable genes across time identified marked upregulation of the *valU*, *valX*, *valY*, *lysZ*, *lysQ*, and *lysY* genes, all members of the aminoacyl-tRNA synthesis pathway (Fig. S10), in the DUFA-enriched strain.

In order to understand the effects of these alterations on the *E. coli*

chassis, we compared the most highly significant and differentially abundant transcripts within the *E. coli* genome (here defined as < 0.01 adjusted p [Deseq2] and >3 log fold-change) for the CFA, IBFA, and DUFA strains versus UFA, and compared the shared and unique genes within these sets at 4 h, during mid-log growth phase (Fig. 6a). Over 78% (393) of the high differentially expressed (DE) genes were unique to the DUFA, while there were only 3 genes shared amongst all strains: *ybdL, metF, and metA*. Comparing the genes unique to each comparison, we found that CFA and IBFA each had less than 30 unique DE transcripts compared to UFA, among which were only two transcriptional regulators: *ygeV* (CFA) and *araC* (IBFA) (Fig. 6b). Comparatively, DUFA overexpression resulted in 26 DE transcriptional regulators. There was significant upregulation of genes known to produce stress-related transcriptional cascades such as *soxR/S, marA/R*. We also observed DE in several transcriptional regulators known to affect metal homeostasis, such as overexpression of *fur*, the ferric uptake regulator, and *metJ*, which drives repression of the sulfurous amino acid methionine. Further investigation revealed that the iron acquisition/uptake genes regulated by *fur* were differentially expressed (Fig. S11). Finally, we examined the DE in genes from the central metabolic pathways of glycolysis, citrate (TCA) cycle, and fatty acid biosynthesis for differences between the UFA and the other strains at 4 h (Fig. 6c). As was seen with the differential expression analysis, the DUFA-enriched strain exhibited strong upregulation in these pathways (37 of 89 total genes, or 42%), specifically in TCA cycle genes, including upregulation of the complete *sdh* operon (also a part of the *fur* regulon, see Fig. S11), and downregulation of many genes in the glycolysis pathway. IBFA and CFA production only resulted in upregulation of 17 (19%) and 23 (26%) of genes within the three pathways, respectively.

2.5. Engineering E. coli for production of free IBFAs

To demonstrate these engineered strains are useful for production of non-common FAs, we attempted to engineer the high IBFA content strain (IBFA-5) to produce free IBFAs (FIBFAs). FIBFAs can be readily converted to esters (Kim et al., 2019), alkanes (Schirmer et al., 2010), or alcohols (Jiang et al., 2018) with drastically reduced melting temperature compared to their straight-chain or even terminally-branched counterparts and used as jet fuels or low-temperature lubricants (Bai et al., 2019). Production of FIBFA in engineered microbial hosts have not been previously reported.

FIBFAs can be released from phospholipid by phospholipases that hydrolyze the ester bonds in glycerophospholipids (Ramrakhiani and Chand, 2011). Wild-type *E. coli* has one outer-membrane-bound

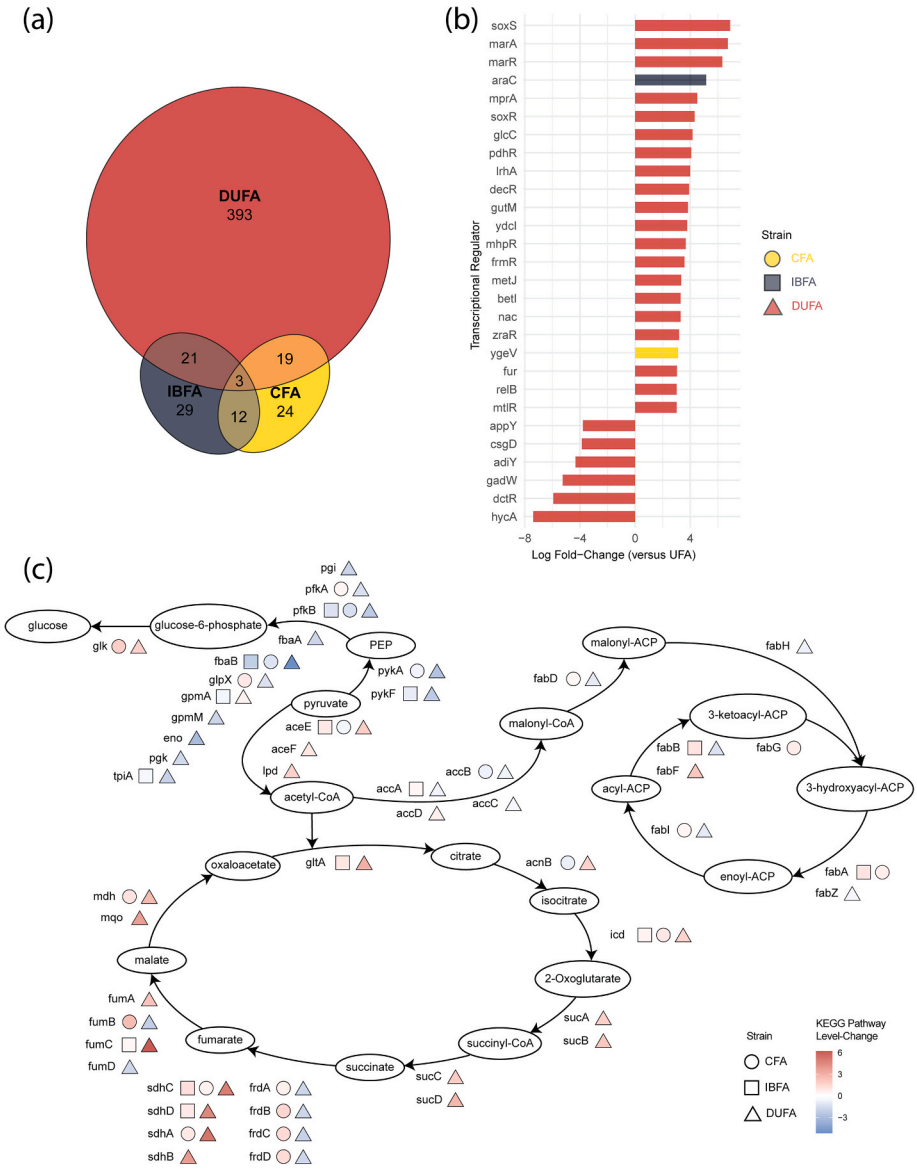

Fig. 6. Transcriptomic profiling of engineered strains with diverse FA profiles. **a**. A Euler diagram showing the intersect and union of the highly DE genes in CFA, IBFA, and DUFA producing strains compared to UFA at 4 h. **b.** Barplot showing the log fold change for every transcriptional regulator within the set of highly DE genes unique to one strain from 6. Color represents the strain they were found to be highly DE in. **c.** Map of differentially expressed genes within the fatty acid biosynthesis, TCA cycle, and glycolysis KEGG pathways. The shapes next to each gene of the pathway represent the three strains, while the color represents the magnitude and direction of differential expression.

phospholipase PldA (encoded by *pldA*) and an inner-membrane-bound phospholipase PldB (encoded by *pldB*, Fig. 7a) (Karasawa and Nojima, 1991). PldA and PldB specifically hydrolyze the FA ester bond at either sn-1 or sn-2 position of phospholipids, respectively (Ramrakhiani and Chand, 2011). Additionally, the inner-membrane-associated phospholipase LipC (encoded by *lipC*) from *B. subtilis* can hydrolyze the FA ester bond at both sn-1 and sn-2 positions (Masayama et al., 2010; Hari et al., 2018). We first separately overexpressed *pldA*, *pldB*, and *lipC* in the IBFA-enriched strain IBFA-5 that contains 40% IBFAs in phospholipids. The fermentation results showed that expression of *pldA*, *pldB*, or *lipC* produced 355.3 mg/L, 150.6 mg/L, and 433.3 mg/L of free FAs (FFAs), respectively, confirming their phospholipase activities (Fig. 7b). While the *pldA*-expressing strain has a slightly higher IBFA fraction in phospholipids (44%, v.s. 40% in the strain without phospholipase overexpression), the *pldB*- and *lipC*-overexpressing strains have lower IBFA fraction in phospholipids (24% and 33%, respectively). This is likely caused by the spatial competition between the methyltransferase BfaB with *pldB* or *lipC* for access to inner membrane phospholipids (Karasawa and Nojima, 1991; Masayama et al., 2010). As inner-membrane-bound or -associated proteins, *pldB* or *lipC* may block BfaB from methylating phospholipids in the cytosolic compartment. When free IBFAs were quantified, while the *pldB*-overexpressing strain failed to produce any FIBFA, the *pldA* and *lipC*-overexpressing strains produced 80 mg/L and 35 mg/L FIBFAs, respectively. Next, *pldA* and *lipC* were coexpressed. Although the titer of total FFAs was increased to 509 mg/L, FIBFA titer was decreased compared to the strain only expressing *pldA*, further suggesting that overexpression of inner-membrane-bound proteins hinder BfaB from methylating phospholipids. Thus, we focus on the strain that only expressed *pldA*.

Next, we targeted to the transmembrane allocation of FFAs. As an outer-membrane enzyme which faces the periplasm, PldA hydrolyzes PE to 2-acylglycerophosphoethanolamine (2-acyl-GPE) and FFAs, both of which could be transported into the cytosol. In the cytosol, acyl-ACP synthetase (AAS, encoded by *aas*), has 2-acylglycerophosphoethanolamine acyltransferase activity and can acylate 2-acyl-GPE back to PE (Hsu et al., 1991; Jackowski and Rock, 1986) (Fig. 7a). To prevent this futile cycle, the *aas* gene was deleted, resulting in increased titers for both FFA (by 29%–507.0 mg/L) and FIBFAs (by 12%–86.9 mg/L) (Fig. 7d). Additionally, periplasmic FFAs can be transferred into the cytosol and simultaneously activated to acyl-CoA by FadD (encoded by *fadD*). Although acyl-CoA cannot be degraded in our engineered strain due to the deletion of the β-oxidation enzyme FadE, it can be incorporated back into the phospholipids in the inner membrane by PlsB and PlsC (Parsons and Rock, 2013; Hsu et al., 1991) (Fig. 7a). To prevent this, *fadD* was also deleted. The resulting strain FIBFA-8 further increased FFAs up to 623.4 mg/L and FIBFAs up to 96.3 mg/L (Fig. 7c).

3. Discussion

In altering the FA-profiles of *E. coli*, we produced significant increases in multiple forms of highly desirable precursor molecules. In addition, we gained substantial knowledge pertaining to the effects of altered FA composition on metabolism, growth, and the transcriptional network of the cell. Increasing ω7-UFA biosynthesis is a necessary precursor to synthesis of CFAs and IBFAs, and thus a similar strategy was applied to all the strains produced in this study: 1) isolating FA biosynthesis from the degradation pathway via deletion of *fadE,* 2) deletion of the native CFA biosynthesis gene, 3) deletion of *fabR*, and 4)

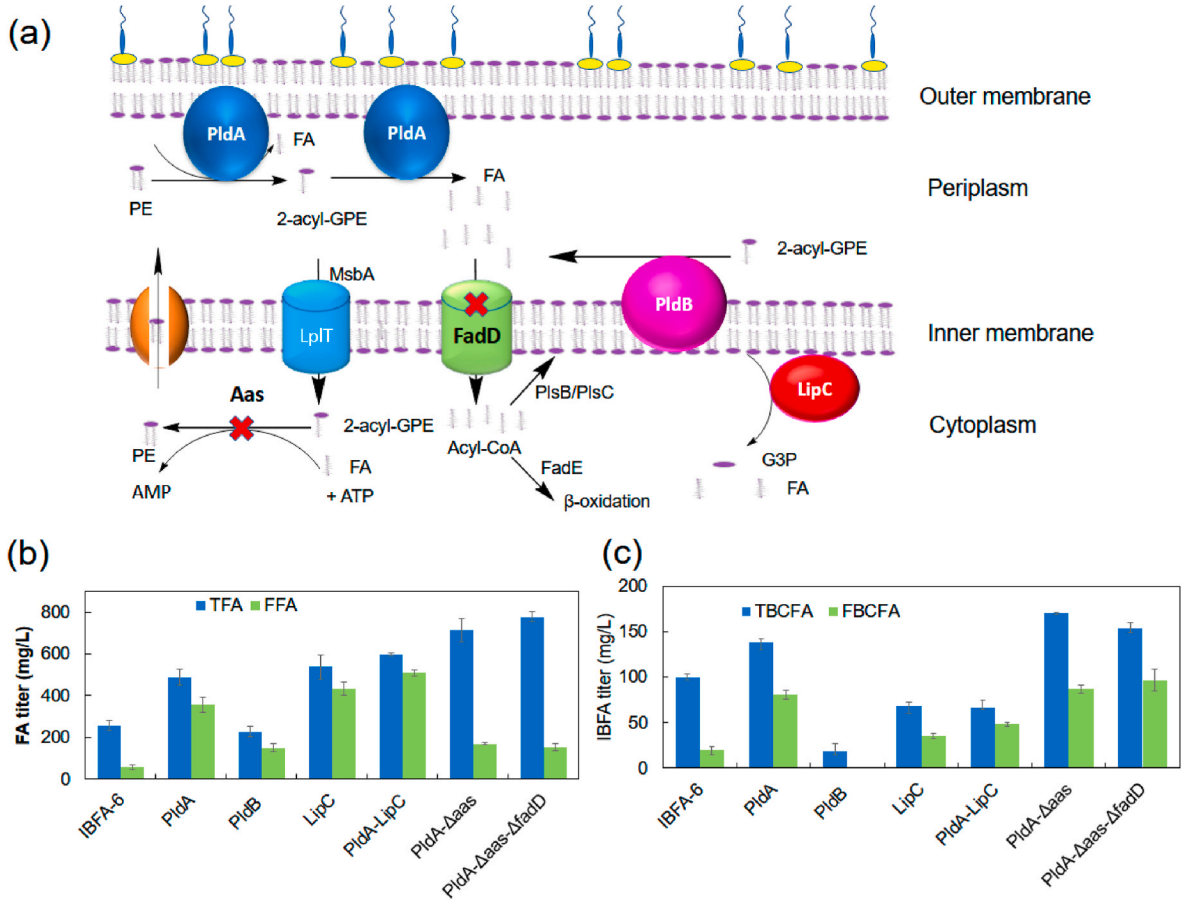

Fig. 7. FIBFA production in engineered *E. coli*. **a**, Metabolic engineering strategies for the production of FIBFAs from phospholipids in *E. coli*. **b**, The titer of total FAs (TFAs) and FFAs in engineered strains. **c**, The titer of total IBFAs (TIBFAs) and FIBFAs in engineered strains. Error bars represent standard deviation measured from biological triplicates.

overexpression of *fadR*, the main transcriptional regulator for FA biosynthesis (Zhang et al., 2012). Surprisingly, overexpression of *fabA* or *fabAB* yielded similar relative proportions of ω7-UFA. The lack of difference between the two suggest that the rate-limiting step of ω7-UFA biosynthesis is catalyzed by FabB, rather than FabA, which is consistent with previous reports (Zhang et al., 2012). Overexpression of *fabB* or *fabR* has been attempted before (Santoscoy and Jarboe, 2021), and in one study produced a similar percentage of total UFA content (Budin et al., 2018); however, it is unclear whether a similar yield of UFA is possible without + *fadB/ΔfabR* in tandem. In the end, deletion of *fabR* alone produced the highest ω7-UFA titers of all engineered strains (Fig. 2a), (Zhang et al., 2012) suggesting that regulatory control of *fabR* is extremely tight and can continue to limit overall FA production even when FA synthesis has been overexpressed. A comparison of our engineering strategies with previous works for increasing UFA fraction is provided in Supplementary Table S7.

Once the MG1655Δ*fadE*Δ*cfa*Δ*fabR* + *fadR* genetic chassis was established, strains optimized for increased CFA, IBFA, and DUFA synthesis were produced by introduction of only two extra genes each. Though cyclopropanation increased the metabolic activity of *E. coli* in multiple tested carbon sources, increased CFA production did not result in improved growth rate when grown in high salt conditions, suggesting overproduction of CFA still imposes a significant burden on the cell when compared to WT; instead, it performed similarly to the other engineered strains. Interestingly, the CFA overproducing strain displayed fewer growth defects compared to strains with increased UFAs and DUFAs (Fig. 5a), yet still displayed a similar expression profile to the UFA strain at all time points (Fig. S9). These results indicate that the expression profile shared by increased UFA, CFA, and IBFA synthesis could be driven by increased energy demand versus FA specific regulation. In turn, the induction of growth defects in the diverse environmental conditions shared by UFA and DUFA overproduction are likely not related to regulation or increased energy demand, but instead to changes in membrane permeability and structure. *E. coli* has been shown to be able to survive on a wide range of UFA as a percentage of total FAs (Sinensky, 1974; Budin et al., 2018). It remains to be seen whether WT *E. coli* strains with higher natural levels of UFA or CFA would better tolerate overproduction of either of these FAs.

Besides the above-mentioned modified FAs in phospholipid membrane, some Gram-positive bacteria can also produce internally IBFAs (Bai et al., 2019; Machida et al., 2017). The best characterized internally IBFA is tuberculostearic acid (TSBA, 10-methylstearic acid) which is found in phospholipids (such as phosphatidylethanolamine, phosphatidylinositol, and diphosphatidylglycerol) and glycolipids (such as phosphatidylinositol mannosides and lipoarabinomannans) in *Mycobacterium tuberculosis* and related species (Lennarz et al., 1962; Bansalmutalik and Nikaido, 2014). Though the biosynthesis mechanism is still not fully understood, it was speculated that TSBA is synthesized from oleic acid by a two-step process of methylenation and reduction, which is catalyzed by an S-adenosyl-L-methionine (SAM)-dependent methyltransferase (BfaB, encoded by *bfaB*) and a FAD-binding oxidoreductase (BfaA, encoded by *bfaA*), respectively (Bai et al., 2019; Machida et al., 2017). However, these two enzyme's direct substrates are still not confirmed. Our analysis of the LC-MS/MS results detected IBFA only in PG, PE, and PS; this suggests that the substrate of the IBFA pathway are likely PS, PE, and PG, but not PA, CDP-DAG, or CL. The significantly higher observed IBFA content in PG compared to PE and PS is likely caused by the dynamic distribution of phospholipids between the inner and outer membrane (Bayer and Bayer, 1985). As the IBFA synthesizing proteins BfaA and BfaB were not predicted to contain any predicted secretion tags or transmembrane sequences (Fig. S11), the IBFA pathway most likely methylates phospholipid FAs in the inner membrane, which then diffuse to the outer membrane. Because PG is enriched in the inner membrane, limits in phospholipid transfer between two membranes can cause a higher IBFA content in PG than that in PS or PE (Bayer and Bayer, 1985). The almost complete conversion of PG from UFA to IBFA at the sn1 position of phospholipids suggests that the IBFA pathway prefers ω7-UFAs at the sn-1. Integration of the IBFA pathway incurred little to no metabolic burden, and the expression profile did not differ from UFA, or CFA, indicative that the *E. coli* chassis was able to integrate a novel phospholipid species. These results also reveal the substrate specificity of IBFA pathway and the distribution of IBFAs in each phospholipid species. Such knowledge can be used to guide future engineering efforts to further tailoring and increasing IBFA content.

Coupling the phenotypic data with the transcriptomic data, we demonstrate the ability of the *E. coli* chassis to tolerate CFA and IBFA induced changes while also not incurring greater metabolic costs. Synthesis of the novel DUFA-enriched strain however, resulted in an altered transcriptional state, decreased stress tolerance as compared to UFA, CFA, and IBFA, and significant metabolic alteration in the host. This resulted in 26 highly DE transcriptional regulators unique to DUFA production, such as redox stress regulating genes *soxR/S* as well as *fur,* the iron regulation repressor, which is itself known to be regulated by *soxR/S*[67](Hantke, 2001). Production of DUFA required overexpression of ferredoxin, and we found many of the iron transport and utilization genes commonly expressed during iron-starvation conditions, such as the *ent, fec, fep,* and *fhu* operons (Seo et al., 2014), to be significantly upregulated. The increased need for iron could be redirecting resources needed for other cellular processes, resulting in activation of the *fur* iron-starvation transcriptional cascade of and the *soxR/S* stress response regulon; *fur* modulate expression of at least 81 gene targets, and indirectly regulates hundreds more (Seo et al., 2014), at the cost of significant intracellular resources. Δ*fur*/Δ*rhyB* has been shown to rescue expression of the *fur* regulated *sdh* TCA cycle genes and *sodB* (Massé and Gottesman, 2002) while also increasing expression of iron uptake and acquisition systems in the presence of iron, and is a possible target for further genetic manipulation to minimize the trade-of between DUFA production and growth.

The cell likely attempts to buffer the changes to FA composition by inducing a natural metabolic response to allow for a similar maximal growth rate during the phenotypic growth assays. Upregulation of the *sdh* operon generates the sRNA *sdhX,* and is theorized to act as a metabolic "overflow" mechanism to shunt acetyl-CoA into acetate for excretion in aerobic conditions in the presence of glucose during high TCA cycle expression (De Mets et al., 2019). Increased *sdh* expression and evidence of overflow metabolism has also been reported in *E. coli* designed for increased FFA production, further defining the important relationship between acetyl-CoA partitioning and the production of FFA (Youngquist et al., 2017). DUFA-enrichment resulted in increased expression of the entire *sdh* operon, likely buffering the metabolic burden of double-bound FA production via the aforementioned mechanism. Overall, though growth rate was affected in some conditions, the *E. coli* chassis largely tolerates DUFA-enrichment and other changes in lipid profiles, while continuing to maintain normal final cell density for all environmental conditions tested.

Future work is needed to elucidate the effects of MUFA- and FIBFA-enrichment on stress tolerance and the transcriptional state of the cell. The initial results indicate that sgRNAs are an excellent method for targeted repression of UFA biosynthesis in *E. coli*; however, more rounds of engineering may further reduce metabolic burden. Alternatively, FIBFA enrichment required the co-expression of two plasmids, and thus likely induces a greater stress on the expression profile of the cell. The use of sophisticated tools such as metabolic flux analysis could identify further refinements for reducing the effects of both increased expression and altered FA profiles on the host (Ando et al., 2018; He et al., 2014).

Overall, this work details the synthetic alterations which enabled the production of altered FA profiles, tailored towards the generation of highly valuable precursor molecules, some of which (*e.g.*, MUFAs, DUFA, IBFAs) have never been produced in the *E. coli* before. We demonstrate that while some of these genetic changes do result in decreased stress tolerance, there is evidence that expression driven regulation of metabolic networks induces a transcriptional response

which allows strains producing UFA, CFA, and IBFA to exhibit a similar expression profile. In addition to creating these novel strains, our work also identified the substrates for the *M. smegmatis* IBFA biosynthesis pathway. This represents a substantial increase in knowledge concerning the effects of FA composition on the bacterial cell, and on the effective generation of high FA-titer producing *E. coli*.

4. Methods

4.1. Reagents

Phusion DNA polymerase was acquired from New England Biolabs (Beverly, MA, USA). Restriction enzymes and T4 DNA ligase were purchased from Thermo Fisher Scientific (Waltham, Massachusetts, USA). Oligonucleotide primers were synthesized by Integrated DNA Technologies (Coralville, IA, USA). Standard 10-methyloctadecanoic acid and 10-methylhexadecanoic acid were purchased from Santa Cruz Biotechnology (Santa Cruz, CA, USA) and Matreya company, (State college, PA, USA), respectively. Bacterial acid methyl ester mixture standards, C4–C24 even carbon saturated FAMEs, GLC-50, GLC-90, and all the other reagents were purchased from Sigma Aldrich (St. Louis, MO, USA).

4.2. Strains and plasmids

All strains and plasmids used in this study are listed in Supplementary Tables 1 and 2 *E. coli* DH10β was used for gene cloning and *E. coli* MG1655Δ*fadE* was used for FA production. *E. coli* and *B. subtilis* genes were amplified from their genome by colony PCR using primers listed in Supplementary Table 3. All other genes were codon-optimized for *E. coli* expression and chemically synthesized by Integrated DNA Technologies (Coralville, IA, USA). All plasmids were constructed using standard Golden-Gate DNA assembly method (Engler et al., 2008). The *cfa*, *fabR, aas* and *fadD* genes were deleted from *E. coli* genome following a CRISPR/Cas9 gene replacement method (Jiang et al., 2015b). All deletions were confirmed by colony PCR. Repression of *fabA* and *fabB* genes was achieved using a CRISPR interference (CRISPRi) method, by expressing constitutively sgRNAs from plasmids (Qi et al., 2013). Plasmids were transformed into electro-competent strains by electroporation and selected on LB agar plates with proper antibiotics (ampicillin, 100 mg/L; kanamycin, 50 mg/L; chloramphenicol, 34 mg/L; spectinomycin 60 mg/L).

4.3. Fermentation

For each transformant, 3 different colonies were selected and used to inoculate 3 ml LB medium with proper antibiotics. The overnight cultures 1% (v/v) were then used to inoculate 20 ml of modified M9 minimal medium (containing 75 mM MOPS at pH7.4, 2 mM $MgSO_4$, 1 mg/Lthiamine, 10 μM $FeSO_4$, 0.1 mM $CaCl_2$ and micro nutrients including 3 μM $(NH_4)_6Mo_7O_{24}$, 0.4 mM boric acid, 30 μM $CoCl_2$, 15 μM $CuSO_4$, 80 μM $MnCl_2$, and 10 μM $ZnSO_4$) with 2% glucose, 0.5% yeast extract, and corresponding antibiotics in 250 ml flask. When OD_{600} reached 0.6–0.8 at 37 °C, inducer (0.8% Arabinose, 0.5 mM Isopropyl β-D-1-thiogalactopyranoside(IPTG), 2 μM anhydrotetracycline) was added and the cell cultures were grown at 18 °C for 48 h (ω7-UFA, CFA, DUFA) or 30 °C for 24 h (Δ5-MUFA, IBFA). After fermentation, cells were harvested for FA quantification.

4.4. Quantification of total FAs

The amount of total FAs was quantified using previously published method (Folch et al., 1957). In detail, 1 ml of cell culture was pelleted and added with 1 ml chloroform, 1 ml of 15% (v/v) H_2SO_4/methanol, and 40 mg/L of nonadecanoic acid as an internal standard and the mixture was heated at 100 °C for an hour for transesterification. Reaction mixture was then cooled on ice for 5 min, followed by the addition of 1 ml purified water followed by vigorous shaking for 1 min (30 s/once, twice). The organic phase containing fatty acid methyl esters (FAMEs) was isolated and directly analyzed using a gas chromatograph (GC) (Hewlett-Packard model 7890 A, Agilent Technologies) equipped with a 30 m DB5-MS column (J&W Scientific) and a mass spectrometer (5975C, Agilent Technologies) or a Flame Ionized Detector (FID) (Agilent Technologies). The column was equilibrated at 80 °C for 1 min, followed by a ramp to 300 °C at 20 °C/min, and was then held at 300 °C for 3 min. FA species were identified by comparing their retention times to those of standard FA methyl esters (Bacterial Acid Methyl Ester Mix, Sigma Aldrich) and by comparing their mass spectra to the Probability Based Matching (PBM) Mass Spectrometry Library. C18:2, Δ5Δ11 was identified by comparing GC-MS spectra of efedrenic acid methyl ester to the published spectra (Bonamore et al., 2006). FA concentrations were quantified by comparing the area of each FAME peak to a standard curve generated using standard FAME mixtures (C4–C24 even carbon saturated FAMEs, GLC-50, GLC-90). The titer of FAs for each strain was measured in biological triplicates.

4.5. Quantification of membrane lipids

Membrane lipids were extracted using Bligh and Dyer lipid extraction protocol (Bligh and Dyer, 1959). In detail, cells from 3 ml culture were collected and washed with 0.6% LiCl for 3 times. The pellet was resuspended into 3.8 ml of a $MeOH/H_2O/CHCl_3$ (2:0.8:1, v/v/v) solution, followed by sonication for 30 s on ice. Then, 1 ml $CHCl_3$ and 1 ml 0.63% LiCl were added into the cell lysate. After vigorous shaking for 30 s, the mixture was centrifuged at 800 g for 5 min. The bottom chloroform phase that contains the extracted lipids was transferred into a GC vial using a long Pasteur pipet. The remaining aqueous solution was extracted again using 1 ml of fresh chloroform. To determine the amount of FAs in membrane lipids, the extracted FAs were converted to FAMEs using the above-mentioned method, followed by GC-FID quantification.

4.6. High resolution mass spectrometric analysis of IBFA strain cell membrane

Profiling and structural characterization of phospholipids with high resolution (R = 100,000 at m/z 400) mass spectrometry were performed on a Thermo Scientific (San Jose, CA) LTQ Orbitrap Velos mass spectrometer (MS) with a built-in syringe pump system operated by Xcalibur operating system. A 50 μl/min solvent (methanol with 0.5% NH_4OH) was continuously infused into the ESI source and samples in methanol (10 μl) were flow injected. The skimmer of the ion source was set at ground potential, the electrospray needle was set at 4.0 kV, and temperature of the heated capillary was 300 °C. The automatic gain control of the ion trap was set to 5×10 (Budin et al., 2018), with a maximum injection time of 100 ms. Helium was used as the buffer and collision gas at a pressure of 1×10^{-3} mbar (0.75 mTorr). The MS^n experiments were carried out with an optimized relative collision energy ranging from 25 to 40% and with an activation q value at 0.25. The activation time was set for 10 ms to leave a minimal residual abundance of precursor ion (around 20%). The mass selection window for the precursor ions was set at 1 Da wide to admit the monoisotopic peak to the ion-trap for collision-induced dissociation (CID) for unit resolution detection in the ion-trap or high-resolution accurate mass detection in the Orbitrap mass analyzer. Mass spectra were accumulated in the profile mode, typically for 3–10 min for MS^n spectra (n = 2,3,4). The structural assignments of phospholipid species are based on the MS^n spectra previously described[24 78] (Hsu and Turk, 2009)

4.7. Quantification of FFAs

The concentration of FFAs was determined using the previous published method (Bentley et al., 2016). In detail, 0.5 ml of cell culture was harvested and acidified with 50 μl of 12 N HCl., The mixture was

extracted twice with 0.5 ml ethyl acetate, which was spiked with 20 μg/ml of nonadecanoic acid (C19:0) as an internal standard. FFAs were derivatized to FAMEs by adding 90 μl methanol, 10 μl 12 N HCl, and 120 μl trimethylsilane-diazomethane. The mixture was incubated at room temperature for 10 min. FAMEs were analyzed using GC-FID.

4.8. Metabolic profiling assays

Colonies from fresh transformation were used to inoculate 3 ml of LB medium with relevant antibiotics and grown at 37 °C overnight. The overnight culture was used to inoculate 5 ml of modified M9 minimal medium supplemented with 2% glucose, 0.5% yeast extract, 0.8% arabinose (inducer) and corresponding antibiotic. Cells were incubated at 18 °C for 42 h (ω7-UFA, CFA, DUFA), or 30 °C for 18 h (WT, IBFA). Cells were diluted 1% in fresh modified M9 and fermentation continued for another 6 h to mid-exponential growth (OD_{600} at 0.6–0.8). For metabolic profiling assays, cells were harvested and washed twice in PBS via centrifugation at 4000 rcf, 2 min, then resuspended in Inoculating Fluid-A (IF-A, Biolog, Hayward, California, USA) with 0.008% arabinose and corresponding antibiotic. Cells were transferred to a GEN III microplate (Biolog, Hayward, California, USA) and cultivated from a starting OD_{600} of 0.01 at 30 °C (for all strains) for 16 h. Absorbance measurements at 590 nm (metabolic activity) and 750 nm (cell growth) were made using an Infinite F200PRO plate reader (TECAN, Männedorf, Switzerland).

4.9. Time course growth assays

For time course growth assays, cells were harvested and washed twice in modified M9 with 0.04 arabinose and 5x antibiotic without any other carbon source. Cells density was normalized to OD_{600} of 0.2, then diluted 5-fold into modified M9 supplemented with carbon, amino acids, and/or harsh condition challenges in a 96-well imaging microplate (Corning, Corning, New York, USA). For cultures with amino acids, the concentrations of the 20 amino acids were standard for EZ rich medium. Plates were measured and incubated in an Infinite F200PRO at 30 °C with 3 mm orbital shaking. Absorbance measurement at 600 nm were made every 10 min for 24 h. Data was imported into R (v4.1.0). Max OD was calculated for each replicate using the max() function in R and averaged across triplicates for each condition. Maximal growth rate was estimated by taking the first derivative of the growth curve and fitting a loess regression. The span which resulted in the lowest sum of squared error was selected for each regression, and the max value of that regression and the confidence interval calculated at that point was used for comparisons between strains.

4.10. Transcriptomics analysis of IBFA-overproducing strain – sample collection

The high IBFA content strain IBFA-5 and the control strain ω7-UFA-5 were cultivated in modified M9 minimal medium as described above. After induction for 4 h, 8 h, and 24 h, 2 ml of cell culture was harvested. Cell pellet was collected by centrifuge at 13,000 g for 2 min, and gently resuspended in 500 μl RNAlater buffer. The resuspension was incubated at room temperature for 20 min and immediately frozen in liquid nitrogen.

4.11. Transcriptomics analysis of IBFA-overproducing strain – RNA extraction and cDNA synthesis

Total genomic material (DNA/RNA) was extracted from frozen cell suspensions using the Quick-RNA fungal/Bacterial Miniprep Kit (Catalog #R2014) from Zymo Research. Cell lysis was conducted using a MiniBeadBeater 24 manufactured by Biospec products for 1.5 min at medium speed. DNA was removed using a modified protocol from the TURBO DNase kit: one round of digestion was immediately followed by spiking in the same amount of DNase and another successive round of heat treatment. Samples were then concentrated and purified using the RNA Clean & Concentrator (Catalog #11–325). Sample total RNA concentrations were measured using a NanoVue (General Electric). We checked for gDNA contamination via PCR of 0.5 μl of sample using a primer sequence designed to target 1640 base pair section of *E. coli gyrA* (Forward: tcttccaggttgatgtctgc, Reverse: tttgcgacctttgaatccgg) samples with pcr products underwent another round of TURBO DNase treatment. We used the Illumina Ribo-Zero Magnetic Kit to deplete rRNA, after which mRNA samples were cleaned and purified using the Agencourt RNAClean XP. First Strand cDNA synthesis was performed using SuperScriptII reverse transcriptase, Second strand cDNA synthesis used *E. coli* DNA polymerase I (New England Biolabs) and RNase H (New England Biolabs) and used *E. coli* ligase (New England Biolabs) and RNase H. Final mRNA concentrations were quantified using the Qubit DNA HS protocol on a Qubit 4 Fluorometer (ThermoFisher). cDNA was stored at −20 °C until sequencing library creation.

4.12. cDNA sequencing

Shotgun metagenomic sequencing libraries were created using cDNA diluted to 0.5 ng/μl and the modifications to the Nextera library prep lot (Illumina) detailed in Baym et al. (2015). This generated ~450 bp DNA fragments which were purified using the Agencourt AMPure XP system (Beckman Coulter) and quantified using the Quant-it PicoGreen dsDNA assay (Invitrogen). Samples were pooled onto lanes to ensure ~10 M (1 × 75bp) reads per sample and quantified using the Qubit dsDNA BR assay. Samples were sequenced in Illumina NextSeq High-output sequencing machines at the Edison Family Center for Genome Sciences and System Biology at Washington University School of Medicine in St. Louis. Sequence data is stored in the National Center for Biotechnology Information (NCBI) Sequence Read Archive (SRA) in bioproject PRJNA762422.

4.13. Transcriptomic analysis

The pipeline for transcriptomic analysis proceeded similarly as previously described (Henson et al., 2018). Briefly, samples were trimmed using trimmomatic and then mapped to a bowtie2 (Langmead and Salzberg, 2012) index built using the *E. coli* MG1655 NCBI assembly GCF_000005845.2_ASM584v2 including a custom plasmidic operon containing the novel biosynthetic pathways for each strain. Gene counts were calculated using featureCounts (Liao et al., 2014). Differential expression analysis was performed using DESeq2 (Love et al., 2014), comparing the UFA-enriched strain as the comparator group for estimating differential expression in the CFA- IBFA- and DUFA-enriched strains. Repeated PERMANOVA conducted in R using the Adonis function of vegan(v2.5-7) (Dixon, 2003) package comparing all timepoints of all strains to each other (999 permutations, Euclidean distance) after rlog normalization in DESeq2. Pathway analysis was conducted using the *Escherichia coli* K-12 MG1655 KEGG pathway gene lists, and testing for significant log fold-change in expression among triplicates using DESeq2.

Author contribution

F.Z., W.B., W.E.A., and G.D. conceived the project. W.B. and S.W. engineered the microbial strains, performed fermentation, and FA analysis; F.H. performed the lipid analysis; C.H. performed phenotypic profiling and growth experiments; W.E.A. performed the transcriptomic analysis. All authors analyzed the data and wrote the paper.

Competing financial interests

The authors claim no competing financial interests.

Acknowledgements

This work was supported by the Department of Energy (DESC0018324).

Appendix A. Supplementary data

Supplementary data to this article can be found online at https://doi.org/10.1016/j.ymben.2022.08.011.

References

Abraham, J., 1995. Domb, Raphael & Nudelman biodegradable polymers derived from natural fatty acids. J. Polym. Sci. Polym. Chem. 33, 717–725.
Akhtar, M.K., Turner, N.J., Jones, P.R., 2013. Carboxylic acid reductase is a versatile enzyme for the conversion of fatty acids into fuels and chemical commodities. Pnas 110, 87–92.
Altabe, S.G., Aguilar, P., Caballero, G.M., Mendoza, D.D., 2003. The Bacillus subtilis acyl lipid desaturase is a Δ5 desaturase. J. Bacteriol. 185, 3228–3231.
Dixon, P., 2003. Vegan, A package of R functions for community ecology. J. Veg. Sci. 14, 927–930.
Ando, D., Garcia Martin, H., 2018. In: Jensen, M.K., Keasling, J.D. (Eds.), Synthetic Metabolic Pathways: Methods and Protocols. Springer New York, New York, NY, pp. 333–352.
Bai, W., Geng, W., Wang, S., Zhang, F., 2019. Biosynthesis, regulation, and engineering of microbially produced branched biofuels. Biotechnol. Biofuels 12, 84.
Bansalmutalik, R., Nikaido, H., 2014. Mycobacterial outer membrane is a lipid bilayer and the inner membrane is unusually rich in diacyl phosphatidylinositol dimannosides. Proc. Natl. Acad. Sci. U. S. A. 111, 4958–4963.
Bayer, M.H., Bayer, M.E., 1985. Phosphoglycerides and phospholipase C in membrane fractions of *Escherichia coli* B. J. Bacteriol. 162, 50–54.
Baym, M., et al., 2015. Inexpensive multiplexed library preparation for megabase-sized genomes. PLoS One 10, e0128036.
Bentley, G.J., Jiang, W., Guaman, L.P., Xiao, Y., Zhang, F., 2016. Engineering *Escherichia coli* to produce branched-chain fatty acids in high percentages. Metab. Eng. 38, 148–158.
Bligh, E.G., Dyer, W.J., 1959. A rapid method of total lipid extraction and purification. Can. J. Biochem. Physiol. 37, 911–917.
Bonamore, A., Macone, A., Colotti, G., Matarese, R.M., Boffi, A., 2006. The desaturase from Bacillus subtilis, a promising tool for the selective olefination of phospholipids. J. Biotechnol. 121, 49–53.
Bowen, C.H., Bonin, J., Kogler, A., Barba-Ostria, C., Zhang, F., 2016. Engineering *Escherichia coli* for conversion of glucose to medium-chain omega-hydroxy fatty acids and alpha,omega-dicarboxylic acids. ACS Synth. Biol. 5, 200–206.
Budin, I., et al., 2018. Viscous control of cellular respiration by membrane lipid composition. Science 362, 1186–1189.
Cao, Y., Yang, J., Xian, M., Xu, X., Liu, W., 2010. Increasing unsaturated fatty acid contents in *Escherichia coli* by coexpression of three different genes. Appl. Microbiol. Biotechnol. 87, 271–280.
Cao, Y., et al., 2014. Production of free monounsaturated fatty acids by metabolically engineered *Escherichia coli*. Biotechnol. Biofuels 7, 59.
Carroll, A.L., Desai, S.H., Atsumi, S., 2016. Microbial production of scent and flavor compounds. Curr. Opin. Biotechnol. 37, 8–15.
Chang, Y.Y., Cronan, J.E., 1999. Membrane cyclopropane fatty acid content is a major factor in acid resistance of *Escherichia coli*. Mol. Microbiol. 33, 249–259.
Chazarretacifre, L., Martiarena, L., Mendoza, D.D., Altabe, S.G., 2011. Role of ferredoxin and flavodoxins in Bacillus subtilis fatty acid desaturation. J. Bacteriol. 193, 4043–4048.
Cronan Jr., J.E., 1968. Phospholipid alterations during growth of *Escherichia coli*. J. Bacteriol. 95, 2054–2061.
Cronan Jr., J.E., 2002. Phospholipid modifications in bacteria. Curr. Opin. Microbiol. 5, 202–205.
Cronan, J.E., Gelmann, E.P., 1973. An estimate of the minimum amount of unsaturated fatty acid required for growth of *Escherichia coli*. J. Biol. Chem. 248, 1188–1195.
Cronan Jr., J.E., Nunn, W.D., Batchelor, J.G., 1974. Studies on the biosynthesis of cyclopropane fatty acids in *Escherichia coli*. Biochim. Biophys. Acta Lipids Lipid. Metabol. 348, 63–75.
De Mets, F., Van Melderen, L., Gottesman, S., 2019. Regulation of acetate metabolism and coordination with the TCA cycle via a processed small RNA. Proc. Natl. Acad. Sci. USA 116, 1043.
Dunlop, M.J., 2011. Engineering microbes for tolerance to next-generation biofuels. Biotechnol. Biofuels 4, 32.
Dunlop, M.J., Keasling, J.D., Mukhopadhyay, A., 2010. A model for improving microbial biofuel production using a synthetic feedback loop. Syst Synth Biol 4, 95–104.
Engler, C., Kandzia, R., Marillonnet, S., 2008. A one pot, one step, precision cloning method with high throughput capability. PLoS One 3, e3647.
Falls, K.C., Williams, A.L., Bryksin, A.V., Matsumura, I., 2014. *Escherichia coli* deletion mutants illuminate trade-offs between growth rate and flux through a foreign anabolic pathway. PLoS One 9 e88159-e88159.
Feng, Y., Cronan, J.E., 2009. *Escherichia coli* unsaturated fatty acid synthesis: complex transcription of the fabA gene and in vivo identification of the essential reaction catalyzed by FabB. J. Biol. Chem. 284, 29526–29535.
Folch, J.M.S., M, L.M., Stanley, G.H.S., 1957. A simple method for the isolation and purification of total lipids from animal Tissues. J. Sci. Food Agric. 22, 24–36.
Goh, E.B., Baidoo, E.E., Keasling, J.D., Beller, H.R., 2012. Engineering of bacterial methyl ketone synthesis for biofuels. Appl. Environ. Microbiol. 78, 70–80.
Grogan, D.W., Cronan, J.E., 1997. Cyclopropane ring formation in membrane lipids of bacteria. Microbiol. Mol. Biol. Rev. 61, 429–441.
Hantke, K., 2001. Iron and metal regulation in bacteria. Curr. Opin. Microbiol. 4, 172–177.
Hari, S.B., Grant, R.A., Sauer, R.T., 2018. Structural and functional analysis of E. coli cyclopropane fatty acid synthase. Structure 26, 1251–1258 e1253.
Hawrot, E., Kennedy, E.P., 1978. Phospholipid composition and membrane function in phosphatidylserine decarboxylase mutants of *Escherichia coli*. J. Biol. Chem. 253, 8213–8220.
He, L., et al., 2014. Central metabolic responses to the overproduction of fatty acids in *Escherichia coli* based on 13C-metabolic flux analysis. Biotechnol. Bioeng. 111, 575–585.
Henson, W.R., et al., 2018. Multi-omic elucidation of aromatic catabolism in adaptively evolved Rhodococcus opacus. Metab. Eng. 49, 69–83.
Hildebrand, J.G., Law, J.H., 1964. Fatty acid distribution in bacterial phospholipids. The specificity of the cyclopropane synthetase reaction. Biochemistry 3, 1304–1308.
Hobby, C.R., et al., 2019. Exogenous fatty acids alter phospholipid composition, membrane permeability, capacity for biofilm formation, and antimicrobial peptide susceptibility in Klebsiella pneumoniae. Microbiology open 8, e00635.
Hsu, F.-F., Turk, J., 2009. Electrospray ionization with low-energy collisionally activated dissociation tandem mass spectrometry of glycerophospholipids: mechanisms of fragmentation and structural characterization. J. Chromatogr. B 877, 2673–2695.
Hsu, L., Jackowski, S., Rock, C.O., 1991. Isolation and characterization of *Escherichia coli* K-12 mutants lacking both 2-acyl-glycerophosphoethanolamine acyltransferase and acyl-acyl carrier protein synthetase activity. J. Biol. Chem. 266, 13783–13788.
Jackowski, S., Rock, C.O., 1986. Transfer of fatty acids from the 1-position of phosphatidylethanolamine to the major outer membrane lipoprotein of *Escherichia coli*. J. Biol. Chem. 261, 11328–11333.
Jiang, W., et al., 2015a. Enhanced production of branched-chain fatty acids by replacing beta-ketoacyl-(acyl-carrier-protein) synthase III (FabH). Biotechnol. Bioeng. 112, 1613–1622.
Jiang, Y., et al., 2015b. Multigene editing in the *Escherichia coli* genome via the CRISPR-Cas9 system. Appl. Environ. Microbiol. 81, 2506–2514.
Jiang, W., Qiao, J.B., Bentley, G.J., Liu, D., Zhang, F., 2017. Modular pathway engineering for the microbial production of branched-chain fatty alcohols. Biotechnol. Biofuels 10, 244.
Jiang, W., Gu, P., Zhang, F., 2018. Steps towards 'drop-in' biofuels: focusing on metabolic pathways. Curr. Opin. Biotechnol. 53, 26–32.
Karasawa, K., Nojima, S., 1991. Lysophospholipases from *Escherichia coli*. Methods Enzymol. 197, 437–445.
Kim, H.M., Chae, T.U., Choi, S.Y., Kim, W., Lee, S.Y., 2019. Engineering of an oleaginous bacterium for the production of fatty acids and fuels. Nat. Chem. Biol. 15, 721–729.
Langmead, B., Salzberg, S.L., 2012. Fast gapped-read alignment with Bowtie 2. Nat. Methods 9, 357–359.
Lee, S.K., Chou, H., Ham, T.S., Lee, T.S., Keasling, J.D., 2008. Metabolic engineering of microorganisms for biofuels production: from bugs to synthetic biology to fuels. Curr. Opin. Biotechnol. 19, 556–563.
Lennarz, W.J., Scheuerbrandt, G., Bloch, K., 1962. The biosynthesis of oleic and 10-methylstearic acids in Mycobacterium phlei. J. Biol. Chem. 237, 664–671.
Lennen, R.M., Pfleger, B.F., 2013. Modulating membrane composition alters free fatty acid tolerance in *Escherichia coli*. PLoS One 8, e54031.
Lennen, R.M., et al., 2011. Membrane stresses induced by overproduction of free fatty acids in *Escherichia coli*. Appl. Environ. Microbiol. 77, 8114–8128.
Liao, Y., Smyth, G.K., Shi, W., 2014. featureCounts: an efficient general purpose program for assigning sequence reads to genomic features. Bioinformatics 30, 923–930.
Love, M.I., Huber, W., Anders, S., 2014. Moderated estimation of fold change and dispersion for RNA-seq data with DESeq2. Genome Biol. 15, 550-550.
Machida, S., Bakku, R.K., Suzuki, I., 2017. Expression of genes for a flavin adenine dinucleotide-binding oxidoreductase and a methyltransferase from Mycobacterium chlorophenolicum is necessary for biosynthesis of 10-methyl stearic acid from oleic acid in *Escherichia coli*. Front. Microbiol. 8, 2061.
Marr, A.G., Ingraham, J.L., 1962. Effect of temperature on the composition of fatty acids in ESCHERICHIA coli. J. Bacteriol. 84, 1260–1267.
Masayama, A., et al., 2010. Bacillus subtilis spore coat protein LipC is a phospholipase B. Biosci., Biotechnol., Biochem. 74, 24–30.
Massé, E., Gottesman, S., 2002. A small RNA regulates the expression of genes involved in iron metabolism in *Escherichia coli*. Proc. Natl. Acad. Sci. USA 99, 4620–4625.
Nawabi, P., Bauer, S., Kyrpides, N., Lykidis, A., 2011. Engineering *Escherichia coli* for biodiesel production utilizing a bacterial fatty acid methyltransferase. Appl. Environ. Microbiol. 77, 8052–8061.
Oyarzún, D.A., Stan, G.-B.V., 2013. Synthetic gene circuits for metabolic control: design trade-offs and constraints. J. R. Soc. Interface 10, 20120671.
Parsons, J.B., Rock, C.O., 2013. Bacterial lipids: metabolism and membrane homeostasis. Prog. Lipid Res. 52, 249–276.
Peralta-Yahya, P.P., Zhang, F., del Cardayre, S.B., Keasling, J.D., 2012. Microbial engineering for the production of advanced biofuels. Nature 488, 320–328.
Qi, L.S., et al., 2013. Repurposing CRISPR as an RNA-guided platform for sequence-specific control of gene expression. Cell 152, 1173–1183.
Ramrakhiani, L., Chand, S., 2011. Recent progress on phospholipases: different sources, assay methods, industrial potential and pathogenicity. Appl. Biochem. Biotechnol. 164, 991–1022.

Richard, D., Kefi, K., Barbe, U., Bausero, P., Visioli, F., 2008. Polyunsaturated fatty acids as antioxidants. Pharmacol. Res. 57, 451–455.
Rowlett, V.W., et al., 2017. Impact of membrane phospholipid alterations in *Escherichia coli* on cellular function and bacterial stress adaptation. J. Bacteriol. 199.
Royce, L.A., Liu, P., Stebbins, M.J., Hanson, B.C., Jarboe, L.R., 2013. The damaging effects of short chain fatty acids on *Escherichia coli* membranes. Appl. Microbiol. Biotechnol. 97, 8317–8327.
Santoscoy, M.C., Jarboe, L.R., 2021. A systematic framework for using membrane metrics for strain engineering. Metab. Eng. 66, 98–113.
Schirmer, A., Rude, M., Li, X., Popova, E., Cardayre, S.B.D., 2010. Microbial biosynthesis of alkanes. Science 329, 559–562.
Seo, S.W., et al., 2014. Deciphering Fur transcriptional regulatory network highlights its complex role beyond iron metabolism in *Escherichia coli*. Nat. Commun. 5, 4910-4910.
Shabala, L., Ross, T., 2008. Cyclopropane fatty acids improve *Escherichia coli* survival in acidified minimal media by reducing membrane permeability to H+ and enhanced ability to extrude H+. Res. Microbiol. 159, 458–461.
Shuntaro, M., Bakku, R.K., Iwane, S., 2017. Expression of genes for a flavin adenine dinucleotide-binding oxidoreductase and a methyltransferase from Mycobacterium chlorophenolicum is necessary for biosynthesis of 10-methyl stearic acid from oleic acid in *Escherichia coli*. Front. Microbiol. 8.
Sinensky, M., 1974. Homeoviscous adaptation–a homeostatic process that regulates the viscosity of membrane lipids in *Escherichia coli*. Proc. Natl. Acad. Sci. U. S. A. 71, 522–525.
Steen, E.J., et al., 2010. Microbial production of fatty-acid-derived fuels and chemicals from plant biomass. Nature 463, 559–562.
Tan, Z., Yoon, J.M., Nielsen, D.R., Shanks, J.V., Jarboe, L.R., 2016. Membrane engineering via trans unsaturated fatty acids production improves *Escherichia coli* robustness and production of biorenewables. Metab. Eng. 35, 105–113.
Tao, H., Guo, D., Zhang, Y., Deng, Z., Liu, T., 2015. Metabolic engineering of microbes for branched-chain biodiesel production with low-temperature property. Biotechnol. Biofuels 8, 92.
Taylor, F.R., Grogan, D.W., Cronan Jr., J.E., 1981. Cyclopropane fatty acid synthase from *Escherichia coli*. Methods Enzymol. 71 Pt C, 133–139.
Willdigg, J.R., Helmann, J.D., 2021. Mini review: bacterial membrane composition and its modulation in response to stress. Front. Mol. Biosci. 8, 634438-634438.
Wolff, R.L., et al., 1999. Δ5-Olefinic acids in the seed lipids from fourEphedraspecies and their distribution between the α and β positions of triacylglycerols. Characteristics common to coniferophytes and cycadophytes. Lipids 34, 855–864.
Yan, Q., Pfleger, B.F., 2020. Revisiting metabolic engineering strategies for microbial synthesis of oleochemicals. Metab. Eng. 58, 35–46.
Youngquist, J.T., Korosh, T.C., Pfleger, B.F., 2017. Functional genomics analysis of free fatty acid production under continuous phosphate limiting conditions. J. Ind. Microbiol. Biotechnol. 44, 759–772.
Zhang, Y., Rock, C.O., 2008. Membrane lipid homeostasis in bacteria. Nat. Rev. Microbiol. 6, 222–233.
Zhang, F., et al., 2012. Enhancing fatty acid production by the expression of the regulatory transcription factor FadR. Metab. Eng. 14, 653–660.